VISIT…

Chapter 11

Hydrodynamic Journal Bearings - Numerical Solutions

Symbols

B_j	bearing number for journal bearings, $\left(\frac{\eta_0 \omega_b r_b b}{\pi w_r}\right)\left(\frac{r_b}{c}\right)^2$
b	width (in side-leakage direction) of journal, m
c	radial clearance of journal bearing, m
c_b	bearing clearance at pad minimum film thickness, m
e	eccentricity of journal, m
h	film thickness, m
$h_{\min}$	minimum film thickness, $c - e$, m
m_p	preload factor
$P_{\max}$	dimensionless maximum film pressure, $\frac{w_r}{2r_b b p_{\max}}$
p	pressure, N/m^2
$p_{\max}$	maximum pressure, N/m^2
p^*	radial load per area, MPa
Q	dimensionless volumetric flow rate, $2\pi q/r_b c b \omega_b$
q	circumferential volumetric flow rate, m^3/s
q_s	side-leakage volumetric flow rate, m^3/s
r_a	radius of shaft, m
r_b	radius of journal bearing, m
Δt_m	temperature change, °C
t_m	absolute temperature, °C
t_{mi}	inlet temperature, °C
$\tilde{u}$	average velocity in sliding direction, m/s
u_b	velocity of journal, m/s
w_r	radial load, N
x, y, z	Cartesian coordinates
α_a	offset factor
ϵ	eccentricity ratio, e/c
η	absolute viscosity, Pa·s
η_0	absolute viscosity at $p = 0$ and constant temperature, Pa·s
λ_j	diameter-to-width ratio, $2r_b/b$
μ	coefficient of sliding friction
Φ	attitude angle, deg
ϕ	cylindrical polar coordinate
$\phi_{\max}$	location of maximum pressure, deg
ϕ_o	location of terminating pressure, deg
ω_b	angular velocity of journal, rad/s

Copyright © 2004 Marcel Dekker, Inc.

11.1 Introduction

The preceding two chapters and this chapter focus on hydrodynamically lubricated journal bearings. Chapter 10 dealt with solutions that could be obtained analytically. These included an infinitely wide journal bearing [applicable for diameter-to-width ratios less than $\frac{1}{2}$ $(\lambda_k = 2r_b/b < \frac{1}{2})$] and short-width journal bearings [applicable for diameter-to-width ratios greater than 2 (*i.e.*, $\lambda_k = 2r_b/b > 2$)]. The present chapter utilizes numerical solutions in obtaining results for the complete range of diameter-to-width ratios. Steady loading conditions are considered throughout most of the chapter, and in the latter part of the chapter dynamic loading effects are considered.

11.2 Operating and Performance Parameters

From Eq. (7.48) the Reynolds equation appropriate when considering the finite journal bearing can be expressed as

$$\frac{\partial}{\partial x}\left(h^3\frac{\partial p}{\partial x}\right) + \frac{\partial}{\partial y}\left(h^3\frac{\partial p}{\partial y}\right) = 12\tilde{u}\eta_0\frac{\partial h}{\partial x} \tag{7.48}$$

Now for a journal bearing $x = r_b\phi$ and $\tilde{u} = u_b/2 = r_b\omega_b/2$.

$$\frac{\partial}{\partial \phi}\left(h^3\frac{\partial p}{\partial \phi}\right) + r_b^2\frac{\partial}{\partial y}\left(h^3\frac{\partial p}{\partial y}\right) = 6\eta_0\omega_b r_b^2\frac{\partial h}{\partial \phi} \tag{11.1}$$

In Chapter 10 the film thickness around the journal is expressed as

$$h = c\,(1 + \epsilon\cos\phi) \tag{10.5}$$

Therefore, Eq. (11.1) can be expressed as

$$\frac{\partial}{\partial \phi}\left(h^3\frac{\partial p}{\partial \phi}\right) + r_b^2 h^3\frac{\partial^2 p}{\partial y^2} = -6\eta_0\omega_b r_b^2 e\sin\phi \tag{11.2}$$

Analytical solutions to Eq. (11.2) are not normally available, and numerical methods are needed. Equation (11.2) is often solved by using a relaxation method. In the relaxation process the first step is to replace the derivatives in Eq. (11.2) by finite difference approximations. The lubrication area is covered by a mesh, and the numerical method relies on the fact that a function can be represented with sufficient accuracy over a small range by a quadratic expression. The Reynolds boundary condition covered in Sec. 10.2.3 is used. Only the results from using this numerical method are presented in this chapter.

The three dimensionless groupings normally used to define the operating parameters in journal bearings are

1. Bearing number (also called Sommerfeld number) for journal bearings,

$$B_j = \left(\frac{\eta_0\omega_b r_b b}{\pi w_r}\right)\left(\frac{r_b}{c}\right)^2 \tag{11.3}$$

Copyright © 2004 Marcel Dekker, Inc.

2. The angular extent of the journal (full or partial)

3. The diameter-to-width ratio $\lambda_j = 2r_b/b$

Recall from Chapter 10 that when the side-leakage term was neglected in Eq. (11.2), λ_k did not exist in the formulation, whereas for the short-width-journal-bearing theory all three parameters occurred although the region of applicability was somewhat limited. The results presented in this chapter are valid for the complete range of operating parameters.

This chapter focuses on the following performance parameters:

1. Eccentricity e

2. Location of minimum film thickness, sometimes referred to as "attitude angle," Φ

3. Friction coefficient μ

4. Total and side flow q and q_s

5. Angle of maximum pressure ϕ_m

6. Location of terminating pressure ϕ_0

7. Temperature rise due to lubricant shearing Δt_m

The parameters Φ, ϕ_m, and ϕ_0 are described in Fig. 11.1, which gives the pressure distribution around a journal bearing. Note from this figure that if the bearing is concentric ($e = 0$), the film shape around the journal is constant and equal to c and no fluid film pressure is developed. At the other extreme, at heavy loads the journal is forced downward and the limiting position is reached when $h_{\min} = 0$ and $e = c$; that is, the journal is touching the bearing.

Temperature rise due to lubricant shearing will be considered in this chapter as was done in Chapter 8 for thrust bearings. In Eq. (11.2) the viscosity of the lubricant corresponds to the viscosity when $p = 0$ but can vary as a function of temperature. Since work is done on the lubricant as the fluid is being sheared, the temperature of the lubricant is higher when it leaves the conjunction than on entry. In Chapter 4 (Figs. 4.5 and 4.6) it was shown that the viscosity of oils drops off significantly with rising temperature. This is compensated for by using a mean of the inlet and outlet temperatures:

$$t_m = t_i + \frac{\Delta t_m}{2} \tag{11.4}$$

where

t_i = inlet temperature
Δt_m = temperature rise of lubricant from inlet to outlet

The viscosity used in the bearing number B_j and other performance parameters is at the mean temperature t_m. The temperature rise of the lubricant from inlet to outlet Δt_m can be determined from the performance charts provided in this chapter.

Copyright © 2004 Marcel Dekker, Inc.

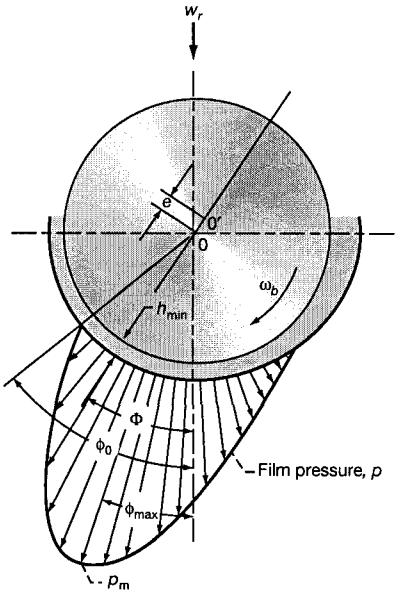

Figure 11.1: Pressure distribution around a journal bearing.

11.3 Design Procedure

Now that the operating and performance parameters have been defined, the design procedure for a hydrodynamic journal bearing can be presented. The results are for a full journal bearing. Results for a partial journal bearing can be obtained from Raimondi and Boyd (1958).

Figure 11.2 shows the effect of the bearing number B_j on the minimum film thickness for four diameter-to-width ratios. The following relationship should be observed:

$$h_{\min} = c - e \tag{11.5}$$

In dimensionless form,

$$H_{\min} = \frac{h_{\min}}{c} = 1 - \epsilon \tag{11.6}$$

where

$$\epsilon = e/c = \text{eccentricity ratio} \tag{11.7}$$

The bearing number for journal bearings is expressed in Eq. (11.3). In a given design the bearing number is affected by

1. Absolute lubricant viscosity η_0
2. Angular shaft speed ω_b
3. Radial load w_r

Copyright © 2004 Marcel Dekker, Inc.

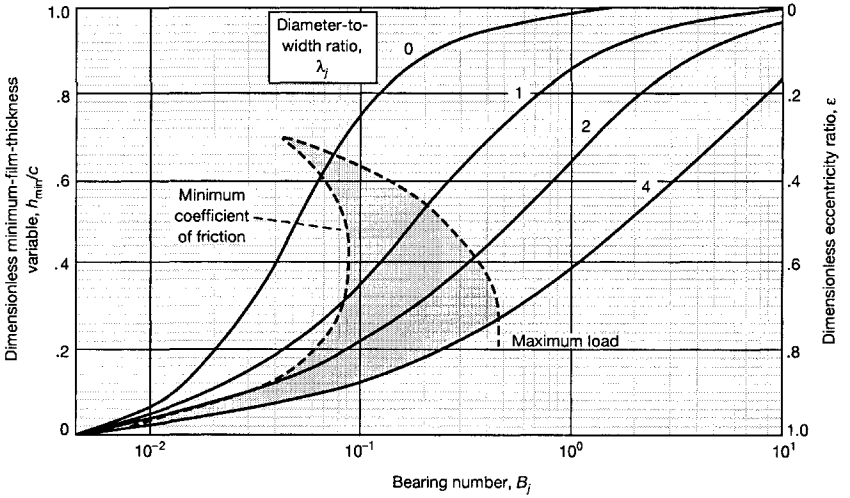

Figure 11.2: Effect of bearing number on minimum film thickness for four diameter-to-width ratios. [*From Raimondi and Boyd (1958).*]

4. Radial clearance c

5. Journal dimensions r_b and b

All these parameters affect the bearing number and thus the design of the journal bearing.

In Fig. 11.2 a recommended operating eccentricity ratio, or minimum film thickness, is indicated as well as a preferred operating area. The left boundary of the shaded zone defines the optimum eccentricity ratio for a minimum coefficient of friction, and the right boundary the optimum eccentricity ratio for maximum load. The recommended operating eccentricity for general application is midway between these two boundaries.

Figure 11.3 shows the effect of the bearing number in the attitude angle Φ [angle between the load direction and a line drawn through the centers of the bearing and journal (see Fig. 11.1)] for four values of λ_j. This angle establishes where the minimum and maximum film thicknesses are located within the bearing. Figure 11.4 shows the effect of the bearing number on the coefficient of friction for four values of λ_j. The effect is small for a complete range of dimensionless load parameters. Figure 11.5 shows the effect of bearing number on the dimensionless volumetric flow rate $Q = 2\pi q/r_b cb\omega_b$ for four values of λ_j. The dimensionless volumetric flow rate Q that is pumped into the converging space by rotating the journal can be obtained from this figure. Of the volume of oil q pumped by the rotating journal, an amount q_s flows out the ends and

Copyright © 2004 Marcel Dekker, Inc.

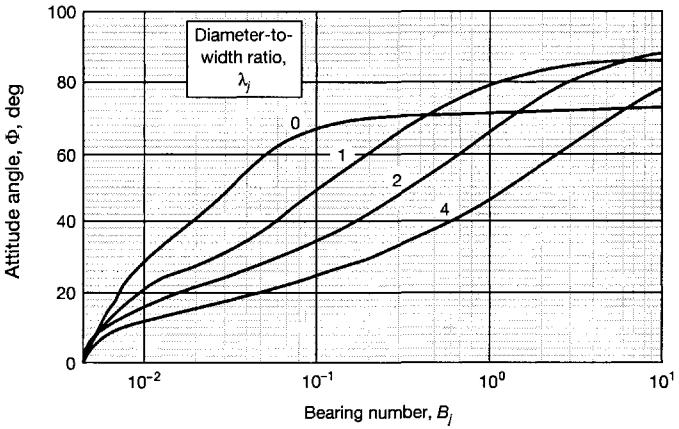

Figure 11.3: Effect of bearing number on attitude angle for four diameter-to-width ratios. [*From Raimondi and Boyd (1958).*]

hence is called *side-leakage volumetric flow.* This side leakage can be computed from the volumetric flow ratio q_s/q of Fig. 11.6.

Figure 11.7 illustrates the maximum pressure developed in a journal bearing. In this figure the maximum film pressure is made dimensionless with the load per unit area. The maximum pressure as well as its location are shown in Fig. 11.1. Figure 11.8 shows the effect of bearing number on the location of the terminating and maximum pressures for four values of λ_j.

The temperature rise in degrees Celsius of the lubricant from the inlet to the outlet can be obtained from Shigley and Mischke (1983) as

$$\Delta t_m = \frac{8.3p^*(r_b/c)\mu}{Q\,(1 - 0.5q_s/q)} \tag{11.8}$$

where $p^* = w_r/2r_b b$ and is in megapascals. Therefore, the temperature rise can be directly obtained by substituting the values of $r_b\mu/c$ obtained from Fig. 11.4, Q from Fig. 11.5, and q_s/q from Fig. 11.6 into Eq. (11.8). The temperature rise in degrees Fahrenheit is given by

$$\Delta t_m = \frac{0.103p^*(r_b/c)\mu}{Q\,(1 - 0.5q_s/q)} \tag{11.9}$$

where

$$p^* = \frac{w_r}{2r_b b} \tag{11.10}$$

and p^* here in Eq. (11.9) is in pounds per square inch.

Once the viscosity is known, the bearing number can be calculated and then the performance parameters can be obtained from Figs. 11.2 to 11.8 and Eqs. (11.9) and (11.10).

Copyright © 2004 Marcel Dekker, Inc.

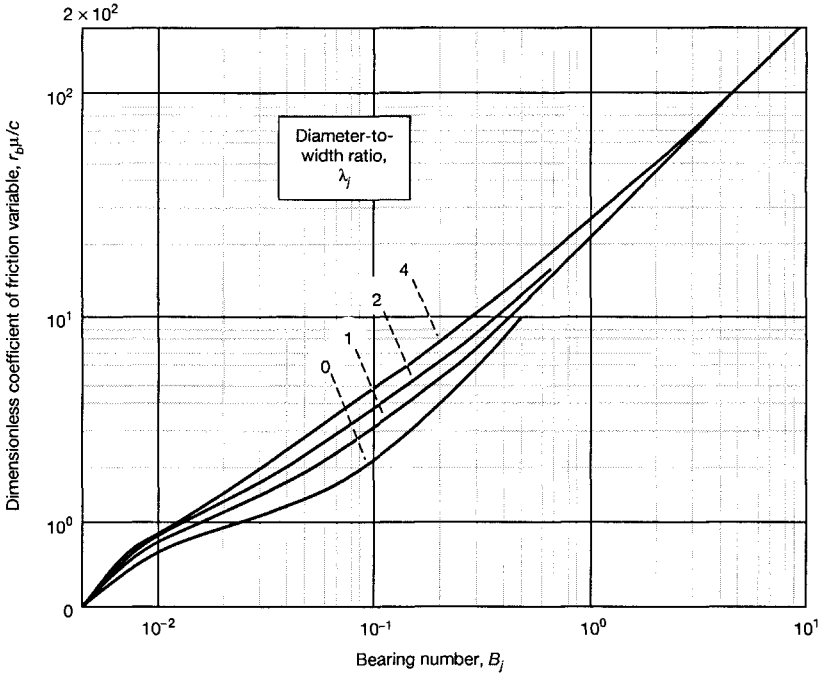

Figure 11.4: Effect of bearing number on friction coefficient for four diameter-to-width ratios. [*From Raimondi and Boyd (1958).*]

The results presented thus far have been for λ_j of 0, 1, 2, and 4. If λ_j is some other value, use the following formula for establishing the performance parameters:

$$\begin{aligned} y &= \frac{1}{(b/2r_b)^3}\left[-\frac{1}{8}\left(1-\frac{b}{2r_b}\right)\left(1-\frac{b}{r_b}\right)\left(1-2\frac{b}{r_b}\right)y_0\right. \\ &+ \frac{1}{3}\left(1-\frac{b}{r_b}\right)\left(1-\frac{2b}{r_b}\right)y_1 - \frac{1}{4}\left(1-\frac{b}{2r_b}\right)\left(1-\frac{2b}{r_b}\right)y_2 \\ &+ \left.\frac{1}{24}\left(1-\frac{b}{2r_b}\right)\left(1-\frac{b}{r_b}\right)y_4\right] \end{aligned} \tag{11.11}$$

where y is any one of the performance parameters ($H_{\min}$, Φ, $r_b\mu/c$, Q, q_s/q, $p_{\max}$, ϕ_0, or $\phi_{\max}$) and where the subscript on y is the λ_j value; for example, y_1 is equivalent to y evaluated at $\lambda_j = 1$. All the results presented are valid for a full journal bearing.

Copyright © 2004 Marcel Dekker, Inc.

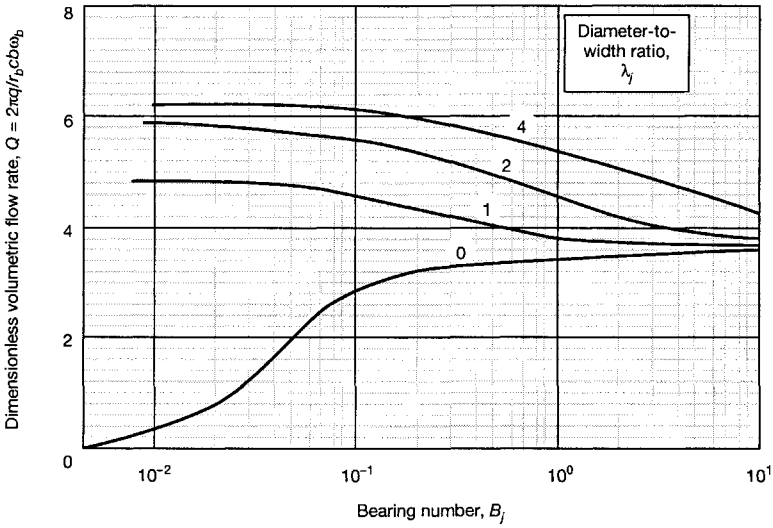

Figure 11.5: Effect of bearing number on dimensionless flow rate for four diameter-to-width ratios. [*From Raimondi and Boyd (1958).*]

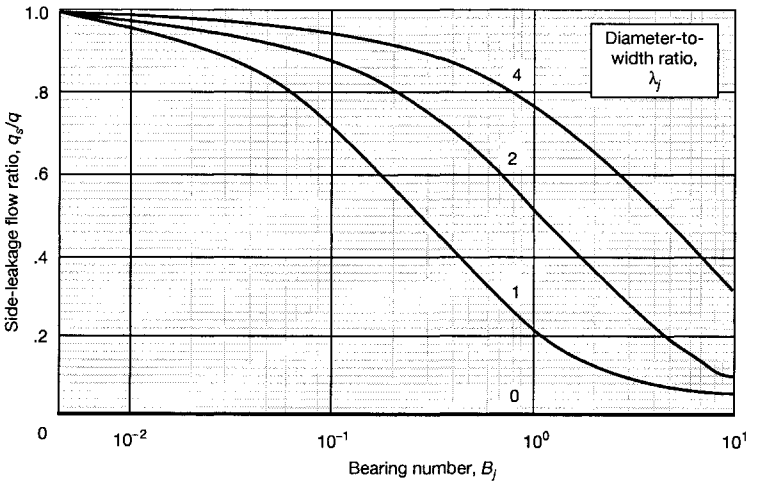

Figure 11.6: Effect of bearing number on volume side flow ratio for four diameter-to-width ratios. [*From Raimondi and Boyd (1958).*]

Copyright © 2004 Marcel Dekker, Inc.

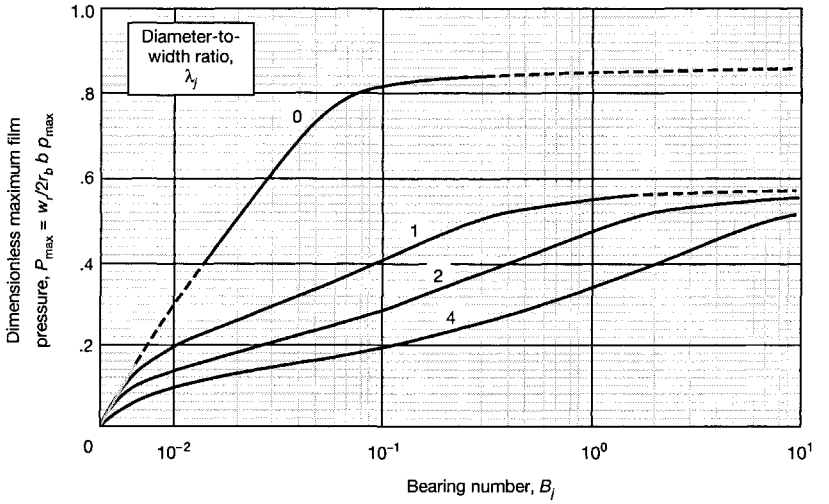

Figure 11.7: Effect of bearing number on dimensionless maximum film pressure for four diameter-to-width ratios. [*From Raimondi and Boyd (1958).*]

Example 11.1

Given A full journal bearing has the specifications of SAE 60 oil with an inlet temperature of 40°C, $N_a = 30$ rps, $w_r = 2200$ N, $r_b = 2$ cm, and $b = 4$ cm.
Find From the figures given in this section establish the operating and performance parameters for this bearing while designing for maximum load.
Solution The angular speed can be expressed as

$$\omega_b = 2\pi N_a = 2\pi(30) = 60\pi \text{ rad/s}$$

The diameter-to-width ratio is

$$\lambda_j = \frac{2r_b}{b} = \frac{2(2)}{4} = 1$$

From Fig. 11.2 for $\lambda_j = 1$ and designing for maximum load

$$B_j = 0.2 \qquad \frac{h_{\min}}{c} = 0.53 \qquad \text{and} \qquad \epsilon = 0.47 \tag{a}$$

For $B_j = 0.2$ and $\lambda_j = 1$ from Figs. 11.4 to 11.6

$$\frac{r_b\mu}{c} = 4.9 \qquad Q = 4.3 \qquad \text{and} \qquad \frac{q_s}{q} = 0.6 \tag{b}$$

Copyright © 2004 Marcel Dekker, Inc.

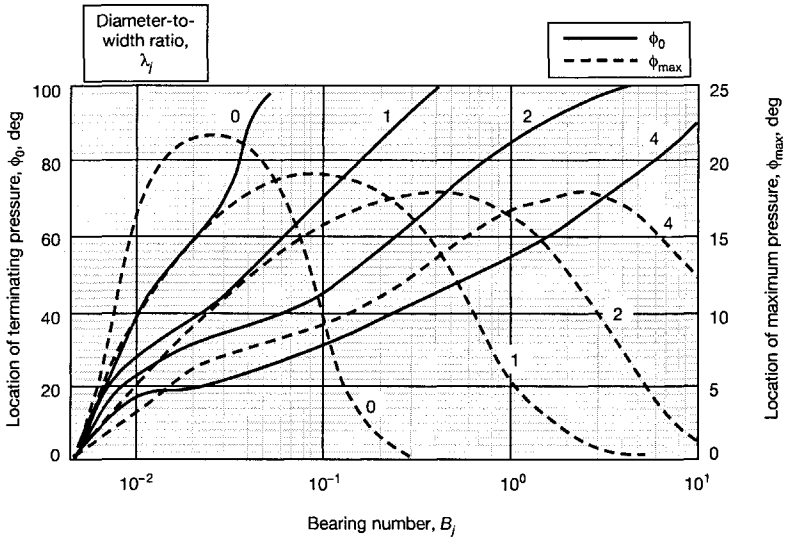

Figure 11.8: Effect of bearing number on location of terminating and maximum pressures for four diameter-to-width ratios. [*From Raimondi and Boyd (1958).*]

From Eq. (11.10) the radial load per area is

$$p^* = \frac{w_r}{2r_b b} = \frac{2200}{2(2)(4)\,(10^{-4})}\ \text{Pa} = 1.375\ \text{MPa} \qquad (c)$$

The lubricant temperature rise in degrees Celsius obtained by using Eq. (11.8) and the results from Eqs. (b) and (c) is

$$\Delta t_m = \frac{8.3p^*\,(r_b/c)\,\mu}{Q\,(1 - 0.5q_s/q)} = \frac{8.3(1.375)(4.9)}{4.3[1 - (0.5)(0.6)]} = 18.58°\text{C}$$

From Eq. (11.4) the mean temperature in the lubricant conjunction is

$$\bar{t}_m = t_{mi} + \frac{\Delta t_m}{2} = 40 + \frac{18.58}{2} = 49.29°\text{C}$$

From Fig. 4.6 for SAE 60 oil at 49.3°C the absolute viscosity is

$$2.5 \times 10^{-5}\ \text{reyn} = 1.70 \times 10^{2}\ \text{centipoise} = 0.170\ \text{N·s/m}^2$$

From Eq. (11.3) the radial clearance can be expressed as

$$c = r_b\sqrt{\frac{\eta_0\omega_b r_b b}{\pi w_r B_j}} = (2)(10^{-2})\sqrt{\frac{(0.170)60\pi(2)(10^{-2})(4)(10^{-2})}{\pi(2.2)(10^3)(0.2)}} = 0.0861{\times}10^{-3}\ \text{m}$$

Copyright © 2004 Marcel Dekker, Inc.

The coefficient of friction from Eq. (b) is

$$\mu = \frac{4.9c}{r_b} = \frac{(4.9)(0.0861)(10^{-3})}{(2)(10^{-2})} = 0.021$$

The circumferential volumetric flow rate is

$$q = \frac{Qr_b cb\omega_b}{2\pi} = \frac{(4.3)(2)(10^{-2})(0.0861)(10^{-3})(4)(10^{-2})60\pi}{2\pi} = 8.89 \times 10^{-6} \text{ m}^3/\text{s}$$

From Fig. 11.3 for $B_j = 0.2$ and $\lambda_j = 1$ the attitude angle is 61°. From Fig. 11.7 for $B_j = 0.2$ and $\lambda_j = 1$ the dimensionless maximum pressure is $P_{\max} = 0.46$. The maximum pressure is

$$p_{\max} = \frac{w_r}{2r_b b P_{\max}} = \frac{2200}{2(2)(10^{-2})(4)(10^{-2})(0.46)} \text{ Pa} = 2.989 \text{ MPa}$$

From Fig. 11.8 for $B_j = 0.2$ and $\lambda_j = 1$ the location of the maximum pressure from the applied load is 18° and the location of the terminating pressure from the applied load is 86°.

11.4 Optimization Techniques

The most difficult of the parameters in the operating conditions to control is the radial clearance c. The radial clearance is difficult to control accurately during manufacturing, and it may increase because of wear. Figure 11.9 shows the performance of a particular bearing calculated for a range of radial clearances and plotted with radial clearance as the independent variable. If the clearance is too tight, the temperature will be too high and the minimum film thickness too low. High temperature may cause the bearing to fail by fatigue. If the oil film is too thin, dirt particles may not pass without scoring or may embed themselves in the bearing. In either event there will be excessive wear and friction, resulting in high temperatures and possible seizing. A large clearance will permit dirt particles to pass through and also permit a large flow of oil. This lowers the temperature and lengthens bearing life. However, if the clearance becomes too large, the bearing becomes noisy and the minimum film thickness begins to decrease again.

Figure 11.9 shows the best compromise, when both the production tolerance and the future wear on the bearing are considered, to be a clearance range slightly to the left of the top of the minimum-film-thickness curve. In this way, future wear will move the operating point to the right, increasing the film thickness and decreasing the operating temperature.

Copyright © 2004 Marcel Dekker, Inc.

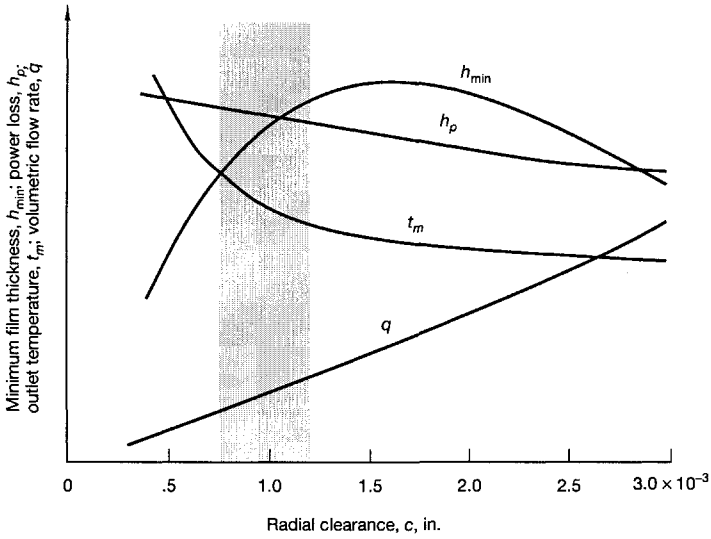

Figure 11.9: Effect of radial clearance on some performance parameters for a particular case.

11.5 Dynamic Effects

The design procedures for steadily loaded journal bearings given in Chapter 10 and thus far in Chapter 11 enable the designer to estimate the performance parameters in terms of the operating parameters. For example, the attitude angle and the eccentricity ratio can be calculated for any steady-state operating condition. From these values the minimum film thickness, a most important quantity affecting the performance of the bearing, can be calculated.

In many important bearing operating situations the load varies in both magnitude and direction, often cyclically. Examples include reciprocating machinery such as diesel and gasoline engines, reciprocating gas compressors, and out-of-balance rotating machinery such as turbine rotors. Bearings are generally dynamically loaded. Furthermore, it must be stressed that journal bearings are not inherently stable. For certain combinations of steady-state operating parameters, self-excited whirl of the journal can be sustained. If this occurs in a case with varying load, the whirl orbit will increase rapidly until the journal and the sleeve come into contact. Journal bearing stability is an important consideration in high-speed rotating machinery, and unstable operation should always be avoided.

Half-frequency whirl occurs if the journal center rotates about the sleeve center at one-half the shaft rotational speed while the eccentricity remains con-

Copyright © 2004 Marcel Dekker, Inc.

stant and the sleeve is stationary. When half-frequency whirl occurs, a constant (zero) pressure exists throughout the bearing. If the shaft precesses about the bearing center at a rotational speed equal to one-half the shaft speed, the theoretical load-carrying capacity is zero and thus the phenomenon is known as "half-speed whirl."

With dynamically loaded journal bearings the eccentricity and the attitude angle will vary throughout the loading cycle, and care must be taken to ensure that the combination of load and speed does not yield a dangerously small minimum film thickness. It is not easy to state a unique value of minimum film thickness that can be assumed to be safe, since a great deal depends on the manufacturing process, the alignment of the machine elements associated with the bearings, and the general operating conditions, including the environment of the machine.

It is also important to recognize the difference between dynamic effects in hydrodynamically lubricated bearings and in rolling-element bearings, which are dealt with in Chapter 22. Although the supporting structure formed by the rolling elements is discontinuous and moving, the bearing as a whole may still be treated as though it were a solid, elastic, springlike element. Spring constants for rolling-element bearings usually fall in the range 1×10^8 to 4×10^8 N/m in the direction of the load application. The rolling elements act in series with the shaft and support stiffnesses and combine according to the reciprocal summation equation. Thus, the dynamic effects as they relate to the fluid film effects in rolling-element bearings are not important and are generally not considered.

Hydrodynamic fluid film bearings are quite another matter, and thus the need for the present chapter. Unfortunately, they cannot be treated as a simple, direct spring. Although the hydrodynamic fluid film bearing does exhibit a springlike resistance that is dependent on journal displacement relative to the sleeve, this force is not linearly related to the displacement nor is it collinear with it. A hydrodynamic fluid film bearing exhibits damping effects that play a very important role in the stability of this type of bearing.

11.6 Nonplain Configurations

Thus far this chapter has focused on plain full journal bearings. As applications have demanded higher speeds, vibration problems due to critical speeds, imbalance, and instability have created a need for journal bearing geometries other than plain journal bearings. These geometries have various patterns of variable clearance so as to create pad film thicknesses that have more strongly converging and diverging regions. Figure 11.10 shows elliptical, offset half, three-lobe, and four-lobe bearings-bearings different from the plain journal bearing. An excellent discussion of the performance of these bearings is provided in Allaire and Flack (1980), and some of their conclusions are presented here. In Fig. 11.10 each pad is moved toward the bearing center some fraction of the pad

Copyright © 2004 Marcel Dekker, Inc.

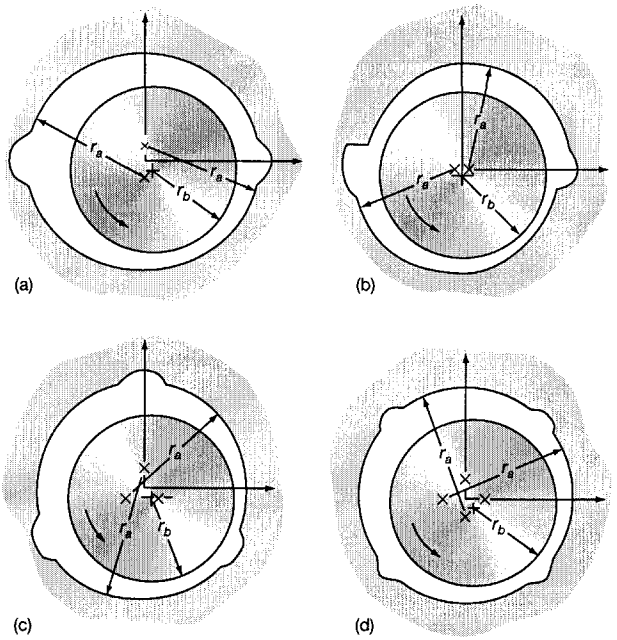

Figure 11.10: Types of fixed-incline-pad preloaded journal bearing and their offset factors α_a. Preload factor m_p, 0.4. (a) Elliptical bore bearing ($\alpha_a = 0.5$); (b) offset-half bearing ($\alpha_a = 1.125$); (c) three-lobe bearing ($\alpha_a = 0.5$); (d) four-lobe bearing ($\alpha_a = 0.5$) [*From Allaire and Flack (1980).*]

clearance in order to make the fluid film thickness more converging and diverging than that occurring in a plain journal bearing. The pad center of curvature is indicated by a cross. Generally, these bearings suppress instabilities in the system well but can be subject to subsynchronous vibration at high speeds. They are not always manufactured accurately.

A key parameter used in describing these bearings is the fraction of length in which the film thickness is converging to the full pad length, called the "offset factor," and defined as

$$\alpha_a = \frac{\text{length of pad with converging film thickness}}{\text{full pad length}}$$

In an elliptical bearing (Fig. 11.10a) the two pad centers of curvature are moved along the vertical axis. This creates a pad with half the film shape converging and the other half diverging (if the shaft were centered), corresponding to an offset factor α_a of 0.5. The offset-half bearing (Fig. 11.10b) is a two-axial-groove bearing that is split by moving the top half horizontally. This results

Copyright © 2004 Marcel Dekker, Inc.

in low vertical stiffness. Generally, the vibration characteristics of this bearing are such as to avoid oil whirl, which can drive a machine unstable. The offset-half bearing has a purely converging film thickness with a converged pad arc length of 160° and the point opposite the center of curvature at 180°. Both the three-lobe and four-lobe bearings (Figs. 11.10c and d) have an α_a of 0.5.

The fractional reduction of the film clearance when the pads are brought in is called the "preload factor" m_p. Let the bearing clearance at the pad minimum film thickness (with the shaft center) be denoted by c_b. Figure 11.11a shows that the largest shaft that can be placed in the bearing has a radius $r_b + c_b$, thereby establishing the definition of c_b. The preload factor m_p is given by

$$m_p = \frac{c - c_b}{c}$$

A preload factor of zero corresponds to all the pad centers of curvature coinciding at the bearing center; a preload factor of 1.0 corresponds to all the pads touching the shaft. Figures 11.11b and c illustrate these extreme situations. For the various types of fixed journal bearing shown in Fig. 11.10 the preload factor is 0.4.

11.7 Closure

The side-leakage term in the Reynolds equation was considered in this chapter for a journal bearing. Analytical solutions to this form of the Reynolds equation are not normally available, and numerical methods are used. When side leakage is considered, an additional operating parameter exists, the diameter-to-width ratio λ_k. Results from numerical solution of the Reynolds equation were presented. These results focused on a full journal bearing, four values of λ_k, and a complete range of eccentricity ratios or minimum film thicknesses. The performance parameters presented for these ranges of operating parameters were

1. Bearing number
2. Attitude angle
3. Friction coefficient
4. Total and side flow
5. Maximum pressure and its location
6. Location of terminating pressure
7. Temperature rise due to lubricant shearing

These performance parameters were presented in the form of figures that can easily be used for designing plain journal bearings. An interpolation formulation

Copyright © 2004 Marcel Dekker, Inc.

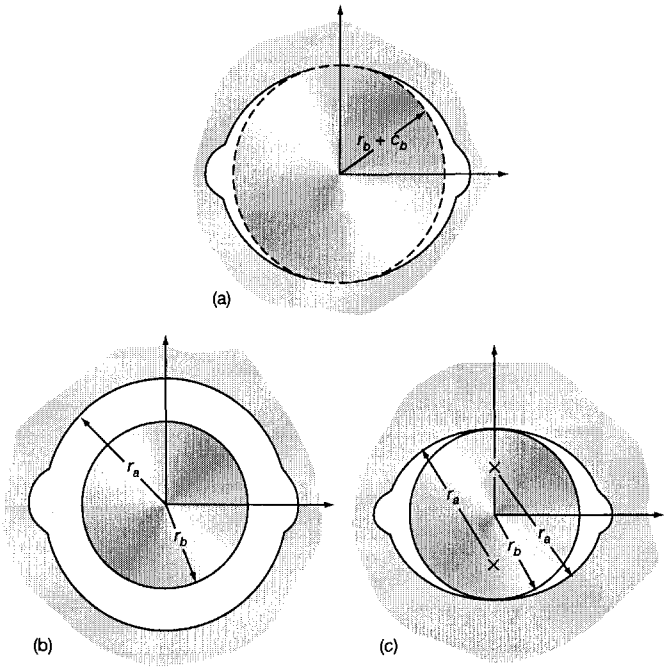

Figure 11.11: Effect of preload factor m_p on two-lobe bearings. (a) Largest shaft that fits in bearing. (b) $m_p = 0$; largest shaft, r_a; bearing clearance $c_b = c$. (c) $m_p = 1.0$; largest shaft, r_b; bearing clearance $c_b = 0$. [*From Allaire and Flack (1980).*]

was provided so that if λ_k is something other than the four specified values, the complete range of λ_k can be considered. Nonplain journal configurations were also considered. It was found that bearing designs with more converging and less diverging film thickness suppressed instabilities of the system. Steady-state and dynamic parameters are given for a plain journal bearing and three nonplain journal bearings.

11.8 Problems

11.1 For the same bearing considered in Example 11.1 determine what the operating and performance parameters are when (a) the half Sommerfeld infinitely-long-journal-bearing theory of Chapter 10 is used and (b) the short-width-journal-bearing theory of Chapter 10 is used. Compare the results.

Copyright © 2004 Marcel Dekker, Inc.

11.2 Describe the process of transition to turbulence in the flow between concentric cylinders when the outer cylinder is at rest and the inner cylinder rotates. How is the process influenced by (a) eccentricity and (b) a superimposed axial flow?

11.3 A plain journal bearing has a diameter of 2 in. and a length of 1 in. The full journal bearing is to operate at a speed of 2000 r/min and carries a load of 750 lbf. If SAE 10 oil at an inlet temperature of 110°F is to be used, what should the radial clearance be for optimum load-carrying capacity? Describe the surface finish that would be sufficient and yet less costly. Also indicate what the temperature rise, coefficient of friction, flow rate, side flow rate, and attitude angle are.

11.4 Discuss the stability of flow between eccentric, rotating cylinders with reference to Rayleigh's criterion. Describe the steps involved in the process of transition to turbulence via the Taylor vortex regime in the flow, and compare the experimentally determined critical Taylor numbers with the results of the Rayleigh criterion analysis.

References

Allaire, P. E., and Flack, R. D. (1980): *Journal Bearing Design for High Speed Turbomachinery in Bearing Design-Historical Aspects, Present Technology and Future Problems.* W. J. Anderson (ed.). American Society of Mechanical Engineers, New York, pp. 111-160.

Lund, J. W. (1979): "Rotor-Bearing Dynamics," Lecture notes. Technical University of Denmark, ISBN 83-04-00267-1.

Raimondi, A. A., and Boyd, J. (1958): A Solution for the Finite Journal Bearing and Its Application to Analysis and Design-I, -11, and -111. *ASLE Trans.*, vol. 1, no. I, I- pp. 159-174; II- pp. 175-193; 111- pp. 194-209.

Shigley, J. E., and Mitchell, L. D. (1983): *Mechanical Engineering Design*, 4th ed. McGraw-Hill, New York.

Copyright © 2004 Marcel Dekker, Inc.